12WCEE 2000

DAMAGE TO A PILE FOUNDATION DUE TO LIQUEFIED GROUND MOTION

Shin'ichiro MORI[1], Atsunori NUMATA[2] And Baoqi GUAN[3]

SUMMARY

During the Hokkaido Nansei-oki, earthquake, July 12, 1993 with magnitude 7.8, extensive liquefaction occurred in reclaimed coastal areas of Hakodate, Japan. A 2500 ton-capacity cement silo at such a liquefied site suffered severe damage with 1/20 tilt, 90 cm differential settlement, and 45 cm lateral displacement. The purpose of this paper is to describe the outline of the damage to the pile foundation of the silo and its surrounding ground, and to elucidate the mechanism of damage by numerical analysis. After the earthquake, various site investigations and laboratory tests were carried out so that the analysis of soil properties and earthquake response analysis by effective stress method based on the results of investigations and tests could clarify that the reclaimed silt layer had liquefied. Furthermore, the excavation survey of all the pile heads and the pipe-camera inspection of several pile shafts were conducted so as to observe the details of pile damages. Finally, in order to study the transient pile stress, nonlinear earthquake response analyses were carried out with modeling the whole soil-pile-structure system to a simple mass-beam-spring system. The analyses results led the authors to conclude that the influence of liquefaction as large deformation of the surrounding ground dominated the pile stresses in pile damage mechanism.

INTRODUCTION

A pile-foundationed cement silo on a coastal reclaimed land in Hakodate city suffered severe damage associated with significant liquefaction due to the 1993 Hokkaido Nansei-oki earthquake of JMA magnitude 7.8 at the epicentral distance of about 170 km. The total damage to the silo was characterized as tilting, differential subsidence and lateral displacement. Excavation survey during the destruction work of silo revealed that all the piles were damaged.

The objective of this paper is to present the outline of damage to the silo, to clarify the detail and mechanism of the damage to pile foundation by field investigation, and to elucidate the causes of damage and the essence of seismic loads by numerical analysis.

2 OUTLINE OF DAMAGE

The location of the damaged silo that existed on a reclaimed land of Hakodate Port is shown in Fig. 1, indicated as KTW (Kita Wharf). In the vicinity of the damaged silo, the liquefaction also caused a silty sand eruption all around the site, whereas one more silo just beside the damaged one did not suffer any damage. Photo. 1 shows the two silos at the site, one is tilted (right) and the other is sound (left); it also shows the tilt of damaged silo and the spreading of erupted silt. The damaged silo with cylindrical structure of 13 m diameter, 26 m high and 2500 tons of capacity was supported on a pile foundation that consisted of 64 prestressed concrete (PC) piles of 40 cm diameter and 22 m length. Its base was a circular plate of 15 m diameter and 1.7 m thickness, and was installed at a depth of 2 m below the ground surface. It was constructed in 1969, just one year after the 1968 Tokachi-Oki

[1] *Department of Civil and Environmental Engineering, Ehime University, Ehime, Japan, E-mail: mori@coe.ehime-u.ac.jp*
[2] *Research Institute of Technology, Tobishima Corporation, Chiba, Japan, E-mail: atsunori_numata@tobishima.co.jp*
[3] *Research Institute of Technology, Tobishima Corporation, Chiba, Japan, E-mail: Baoqi_Guan@tobishima.co.jp*

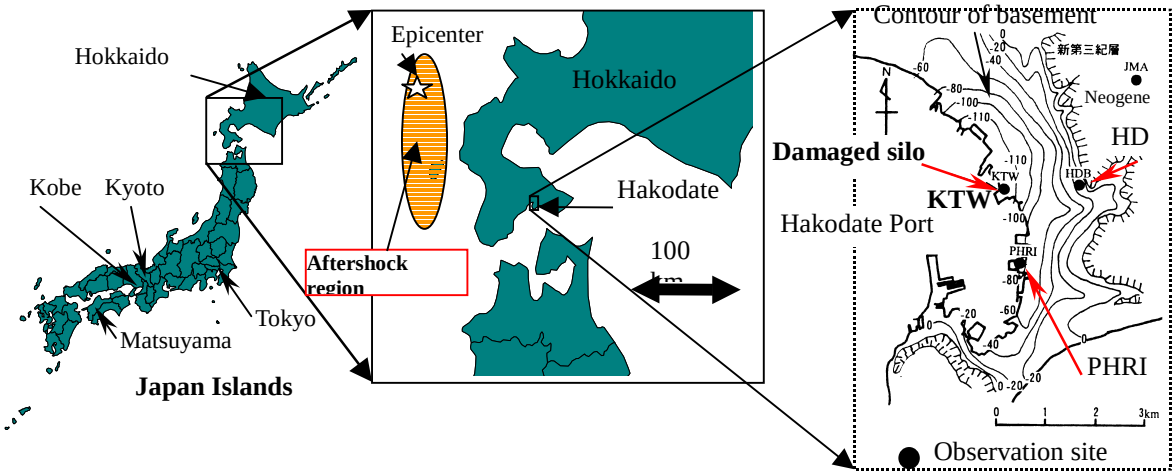

Fig. 1 Location of damaged silo and ground motion observation sites

earthquake attacked the site and caused significant liquefaction, and was designed as per the Design Code of Building Foundation in Japan (1967) without the specifications for pile head connection and lateral seismic loading.

After the 1993 earthquake, the upper structure of the silo subsided by a minimum of 30 cm and a maximum of 90 cm, resulting into differential settlement of 60 cm, tilting of 1/20, and horizontal displacement of 47 cm [Mori et al, 1994]. The direction of tilt and lateral movement was southwest. On the contrary, the other silo that was constructed in 1977 being designed as per the Design Code in 1974 suffered no damage at all.

Photo. 1 Tilted silo (center) and silt eruption

3 DAMAGE TO FOUNDATION PILES

3.1 Damage to pile head

In order to clarify the damage to the pile heads and caps, an investigation by excavation during destruction of the base of the damaged silo was carried out. All the pile heads were exposed out and observed up to 1 to 3 meters below the pile tops. The investigation revealed that all the pile heads were damaged up to a depth of 3 meters, which made it easy to understand the peculiarity that enabled the failure of the pile heads to be classified into two patterns. The failure patterns of the pile heads are illustrated in Figure 2; one is shear failure or bending-shear failure at pile head (to be called Type-A) with large shear deformation and the other is bending failure at a depth of 1 to 3 meters below sound pile top (to be called Type-B) with large tilting.

The distribution of the failure patterns is shown in Fig. 3 where numerals indicate the serial numbers of the piles. The figure makes us to basically understand the mixed and irregular distribution of the two

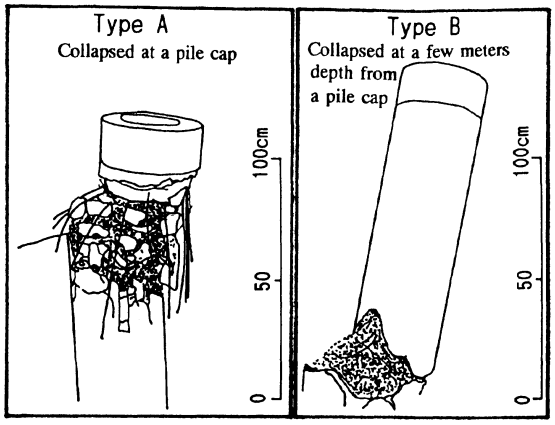

Fig. 2 Failure patterns of damaged pile heads

patterns. Mori and Numata [1999] clarified the causes and mechanism of this peculiarity of the damage by the analyses of the photos taken just after piling in 1969. The two types of failure patterns of the pile heads were distinguished by the ratio of the penetration length, P to the pile diameter, D deciding sufficient connection at pile cap. The criterion of the sufficient ratio, P/D for rigid connection was 0.2. Type-A piles behaved with rigid pile-cap connection due to sufficient penetration, while Type-B piles behaved with pinned connection due to insufficient penetration.

3.2 Damage to pile at a depth

In order to directly observe the damage to the piles at a depth, the internal inspection of PC piles was carried out by inserting a CCD-TV camera into the seven piles with completely failed pile heads. Photo. 2 shows the downward internal view of No.54 pile at a depth. One-meter length of the pile at 6.5 m depth completely failed, and a large shear deformation and longitudinal cracks on the pile were clearly seen. Furthermore, the photo illustrated a lateral shift of half the pile radius at the breakage point due to the shear deformation. The failure patterns and deformations of the 5 piles that had distinct failure are shown in Fig. 4, attached with the soil profile of the site. This figure clearly shows that the piles after failure deformed largely at a depth corresponding to the bottom of reclaimed layer or the top of old sea bottom at the depth of around 7 meters.

3.3 Summary of pile damage

Damage to the piles along the depth is summarized in Fig. 5 (b and c). Damaged portions of the piles were at three different locations: at the pile head, a depth of 1 to 3 meters below the pile cap, and at the depth corresponding to the bottom of the reclaimed layer. The first two locations mean the breakage points of Type-A and Type-B piles as mentioned earlier.

4 SITE AND SOIL CONDITIONS

The surrounding ground of the silo was reclaimed by dredging and filling during 1965 to 1966, which liquefied significantly during the 1968 earthquake, as mentioned earlier. Two times of boring investigation and SPT and a PS logging was carried out after the 1993 earthquake at the site of damaged silo. The soil and SPT N-value profiles of the site, as shown in Fig. 5, consist of a 0.8m thick embankment, a 6m thick dredged-and-filled silt layer with N-value ranging from 2 to 4 (Bk), a 7m thick Holocene silt marine deposit with N-value ranging from 3 to 7 (As1), a 2.8m silty sand layer with N-value ranging from 5 to 13 involving thin stiff sand sub-layer (As2), a 3m thick sandy silt layer with N-value ranging from 8 to 13 (Ac1) and a Pleistocene volcanic ash sand layer with N-value ranging from 20 to

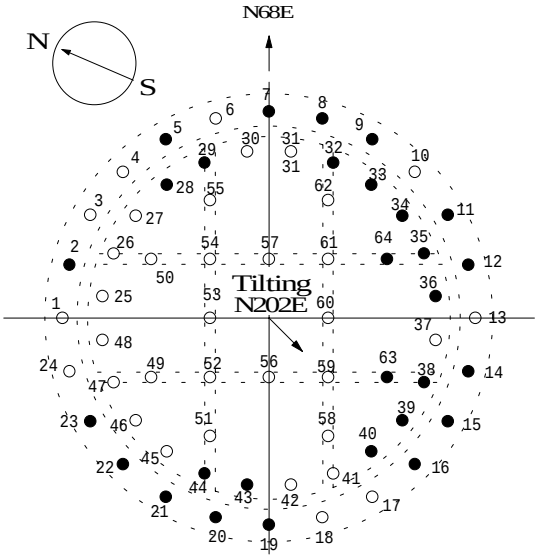

Fig. 3 Distribution of the failure patterns

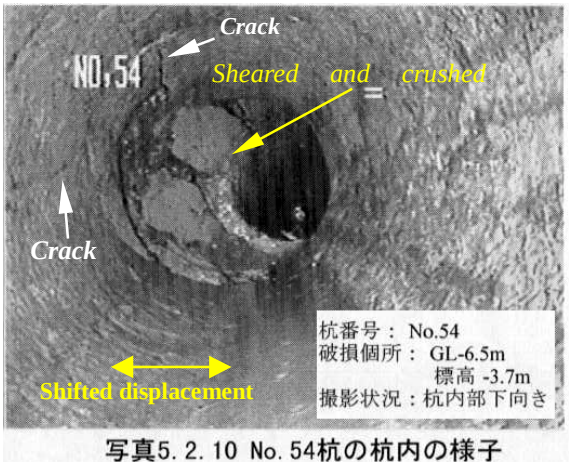

Photo. 2 Downward inner view of the pile No.54 damaged at 6.5 m in depth

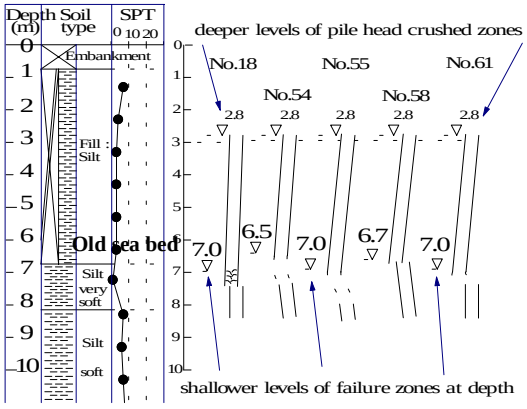

Fig. 4 Pile failures at depth of old sea bottom

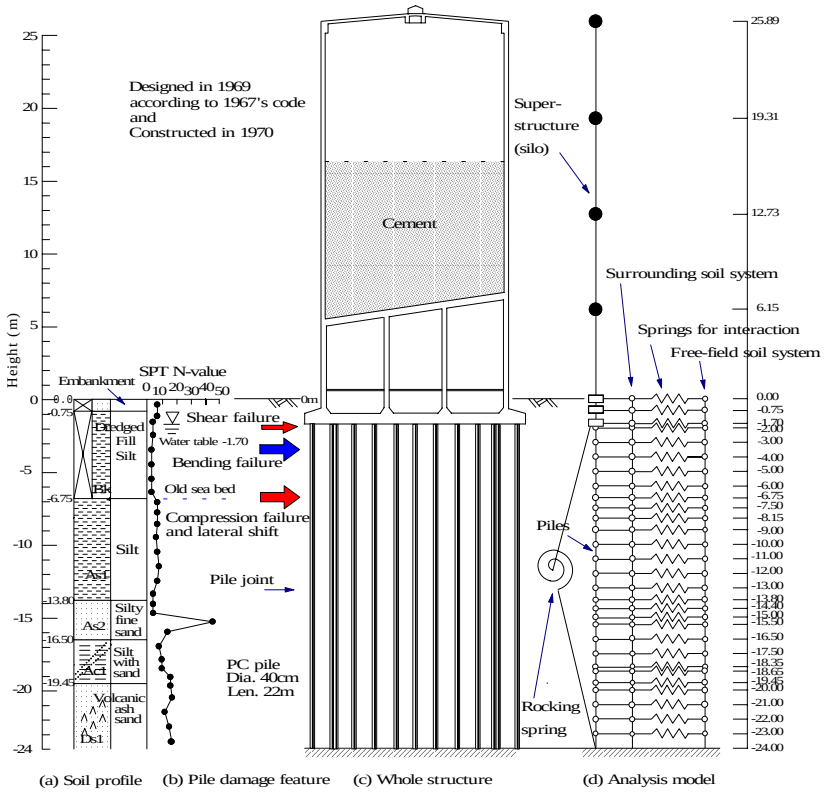

(a) Soil profile (b) Pile damage feature (c) whole structure (d) Analysis model

Fig.5 Soil profile , pile damage portions, silo-pile structure and analysis model

24 continued up to a depth of 30m (Ds1). The values of shear velocity of Bk, As1, As2, Ac1 and Ds1 are 94 to 98, 151, 338, 159, and 222 m/s respectively. The erupted silt was verified to be from the reclaimed layer of soil by particle size analysis (Mori and Numata ,1994)

5 PROCEDURE OF NUMERICAL ANALYSIS OF PILE FOUNDATIONED SILO

5.1 Purpose of analysis

The purposes of the analysis are to elucidate the mechanism of pile damage based on the nonlinear effective analysis with soil-structure interaction (SSI) system, to discuss the influence of liquefaction on the pile response, and to clarify the contribution of inertia force and transient ground displacement. Furthermore, it is intended to verify the applicability of the method proposed by Mori et al. (1992).

5.2 Analysis model

Fig. 5 also shows the dynamic analysis model of SSI system in association with the ground profile and the whole structure of silo and piles. This modeling was the mass-spring system proposed by Mori et al. (1992) with reference to Penzien et al. (1964). The effective analysis of a free field soil column was analyzed by using the effective stress path model developed by Ishihara and Towhata (1980) and the excessive pore water pressure obtained as a result of the analysis was introduced into the model of SSI system. Piles as bending elements were modeled into linear bending-shear beams and the basement into a rigid beam. The columns of the surrounding soil and the free field soil were both modeled into shear spring and mass systems, and the soil-pile interaction into lateral springs. These soil-associated springs were characterized as nonlinear springs with hyperbolic model.

5.3 Input motion

Strong ground motions during main shock of the 1993 earthquake were recorded at HDB (Hokkaido Development Bureau) and PHRI (Port and Harbor Research Institute) sites shown in Fig. 1. After this

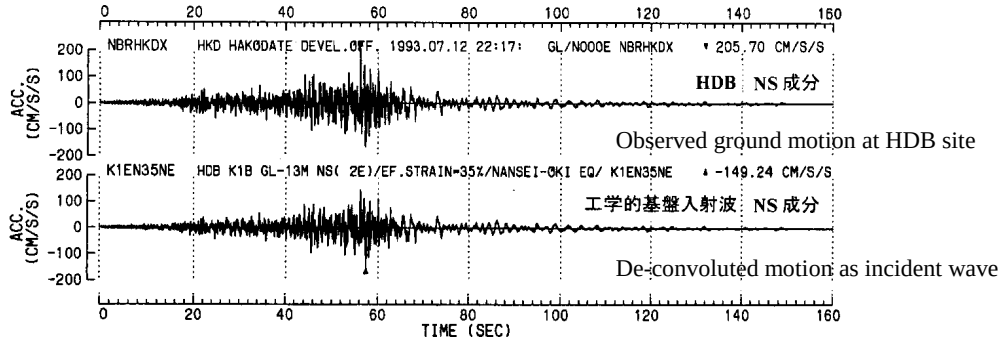

Fig. 6 Observed motion on surface and de-convoluted motion on basement at HDB site

earthquake, accelerometers were also installed at the site of the damaged silo, KTW and the earthquake observation was started. According to the strong motion records obtained simultaneously at the three sites during three large earthquakes for 2 years after the 1993 earthquake, KTW records were similar to HDB rather than PHRI in the range of 0.4 to 2 seconds of response spectra. The input motion in SSI analysis was adopted as the incident wave at the upper end of Ds1 layer obtained through the equivalent linear de-convolution at HDB site by using the acceleration records of the main event. The component of input motion was supposed to be along the north-south direction, since the direction of tilting and movement of damaged silo was. Fig. 6 shows the Observed motion on the surface at HDB site and the de-convoluted motion on the base layer, which was supposed to be the incident wave in the base layer at KTW site. The de-convolution was carried out by using the program SHAKE [Schnabel,P.B. et al., 1972]

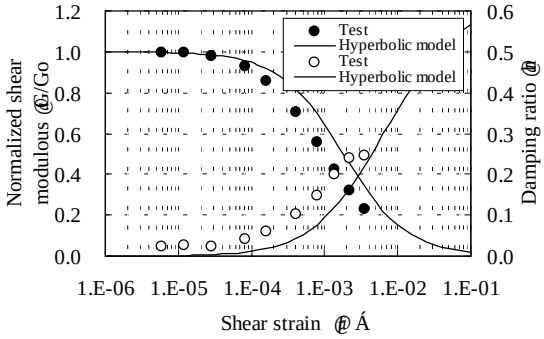

Fig. 8 Dynamic characteristics of soil (16th sublayer element)

5.4 Determination of model parameters

Model parameters of soil and interaction springs were determined by using the results of SPT, PS logging, and laboratory tests with undisturbed samples (dynamic deformation test, undrained cyclic shear test, and CD test carried out with triaxial apparatus). Fig. 7 shows the comparison of the strain-dependent dynamic deformation characteristics by test and hyperbolic model. The hyperbolic model requires two parameters, G_{max} and τ_{max}. G_{max} was determined with shear velocity, Vs and density, ρ, and τ_{max} as $\sigma_v' \tan\phi$, where σ_v' is the initial effective overburden pressure and ϕ is the internal friction angle of soil.

The parameters of the effective stress path mode were determined with laboratory test results according to the proposed method by Ishihara and Towhata (1980). Liquefaction resistance characteristics of reclaimed silt layer (Bk) are shown in Fig. 8. This figure shows a comparison between the test results of undisturbed samples and those of the numerical simulation by the effective path model with determined parameters. Good agreement between test and analysis results can be seen.

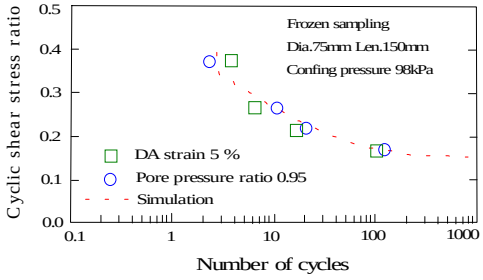

Fig. 9 Comparison between test and simulation in liquefaction resistance

5.5 Soil-pile interaction springs and rocking spring

There are two parameters of soil-pile interaction spring; one is the tangent modulus at infinite small strain, K_{max} and the other is the ultimate strength, F_{max}. These parameters were determined as : At first for a single pile, K_{max} was determined by calculations using Mindlin's second solutions and F_{max} was determined as 3 times the passive earth pressure on projected area of pile. Secondary for pile group, $(1/n)^{1/2}$ as the factor of efficiency of pile group, where n is number of piles, was multiplied by the parameters for a single pile both on K_{max} and F_{max} as well as multiplied by n.

Rocking spring was basically modeled with 3 components of pile, its surrounding soil and its bearing basement.

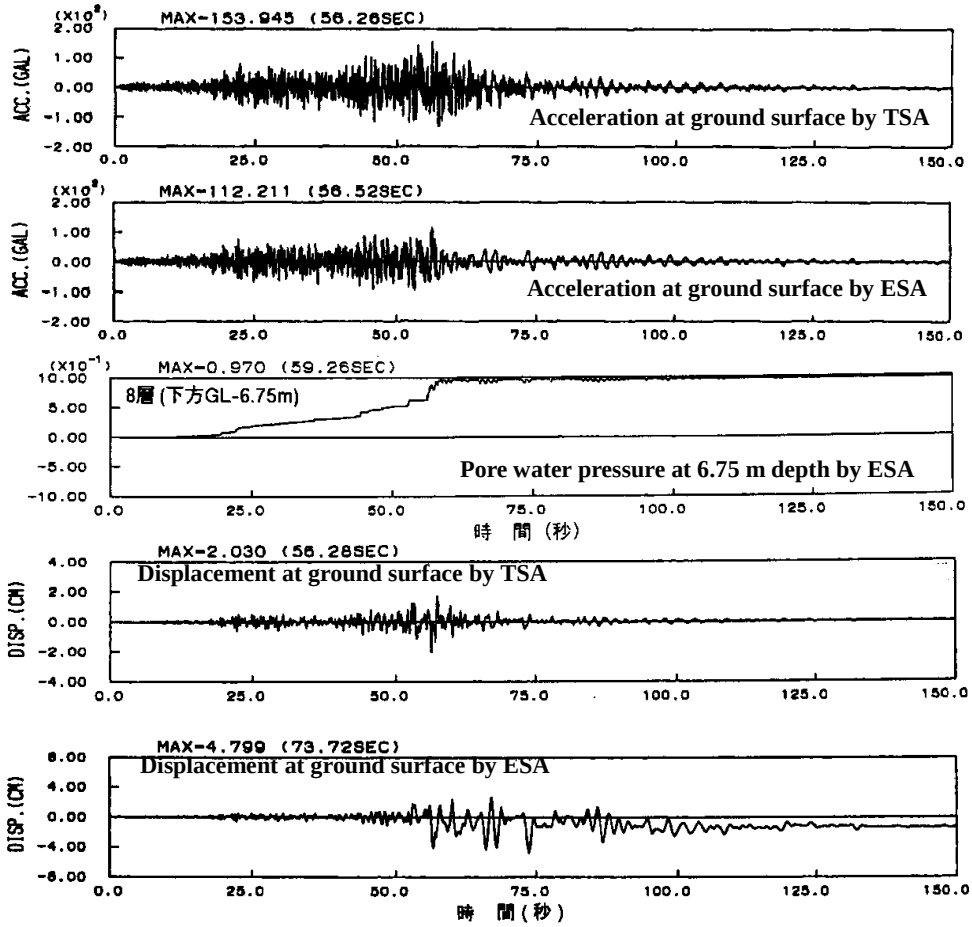

Fig. 9 Time histories of acceleration and displacement responses at ground surface both by effective stress analysis (ESA) and total stress analysis (TSA), and the time history of excessive pore water pressure in a depth of 6.75 m by ESA

Pile and its surrounding soil were connected in parallel, while pile and its bearing basement were connected in series.

5.6 Damping

Rayleigh damping was adopted. The coefficients α and β for Rayleigh damping ([C]= α [M]+ β [K]) were determined so as to have 4 % of damping ratios at the predominant frequencies of first and second vibrational modes of ground as 1.8 and 4.3 Hz respectively.

6 RESULTS OF DYNAMIC ANALYSIS AND THEIR CONSIDERATION

6.1 Acceleration and displacement responses at ground surface

The time histories of acceleration and displacement responses at ground surface both with effective stress analysis (ESA) and total stress analysis (TSA), and the time history of excessive pore water pressure in a depth of 6.75 m by ESA are shown in Fig. 9. Difference between ESA and

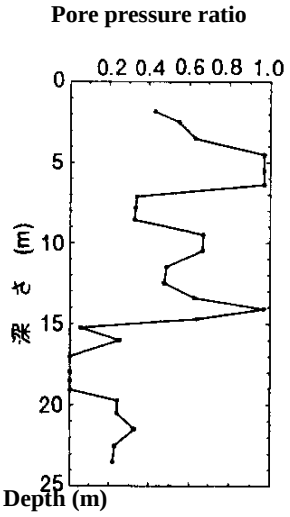

Fig. 10 Distribution of pore water pressure ratio along depth

TSA before 45 seconds is observed to be very small. On the contrary, after 53 seconds, the amplitude of acceleration decreases and the higher components of displacement diminish in the results of ESA compared with those of TSA. Furthermore, after 56 seconds when excessive pore pressure reaches the maximum of 97 %, it can be clearly seen and understood that the amplitude of acceleration suddenly decreases and that of displacement suddenly increases. In addition, south-directed residual displacement at ground surface can be seen.

6.2 Excessive pore water pressure response

The profile of excessive pore water pressure ratio is shown in Fig. 10. This figure explains that complete liquefaction was spread along the depth of 4 to 6 m in reclaimed silt layer and the pore pressure in the upper part of As1 layer and in a part of As2 layer reached a considerable level.

6.3 Bending moment of pile and influence of liquefaction

The distributions of the bending moment of pile in two cases of pile-cap connecting condition are shown in Fig. 11. This figure contains the result of TSA (a) and ESA (b). In the case of TSA, the value at pile head with rigid connection reaches the amount of cracking moment, whereas the value at a depth of 3 m with pinned connection reaches 80 % of cracking moment. The depth of maximum bending moment in the case of pinned connection depends on the interaction spring, accordingly the result of TSA can explain Type-B failure. Meanwhile, the actual input motion might be larger than that considered in the analysis. If so, the pile head with rigid connection might have failed even without the liquefaction, which means that the result of TSA can explain Type-A failure. On the other hand, in the case of ESA, the depth of maximum bending moment in the case of pinned connection is 6 to 7 m, which coincides with the depth of shear failure in the actually damaged piles. Furthermore, the value at pile head with rigid connection in case of ESA reaches 1.5 times of that of TSA and is beyond the ultimate strength. This result harmonizes the actual feature of Type-A failure. Fig. 12 shows, in the space of bending moment and axial forces, the response path at pile cap in the case of rigid connection and the yield surface. The response of TSA model exceeds the crack line only once but never reaches the yield surface, whereas that of ESA model passes beyond the line over and over again, and then reaches the yield surface. Therefore, the ESA model can preferably explain the whole feature of pile damage; so, liquefaction considerably contributes to causing damage to the pile head.

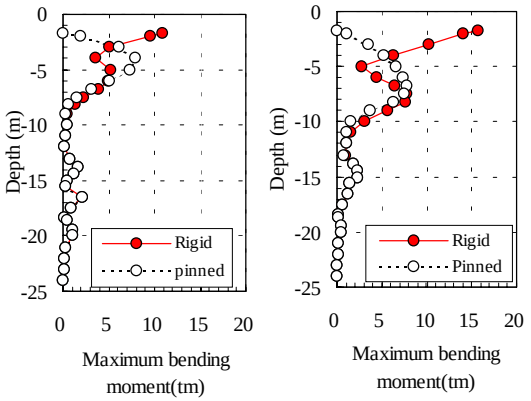

(a) Total stress analysis (b) Effective stress analysis

Fig. 11 Distributions of the bending moment of pile in two cases of pile-cap connecting condition

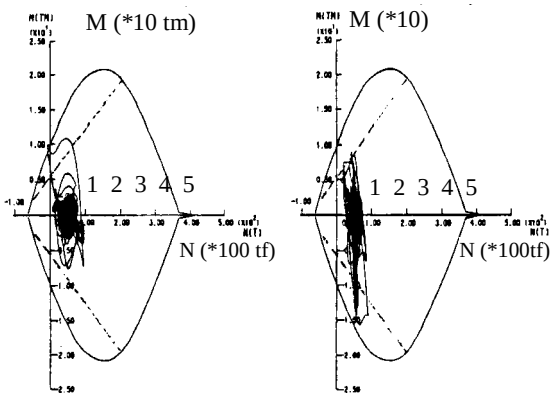

Fig. 12 Response path at pile cap in the case of rigid connection and the yield surface in the space of bending moment and axial forces

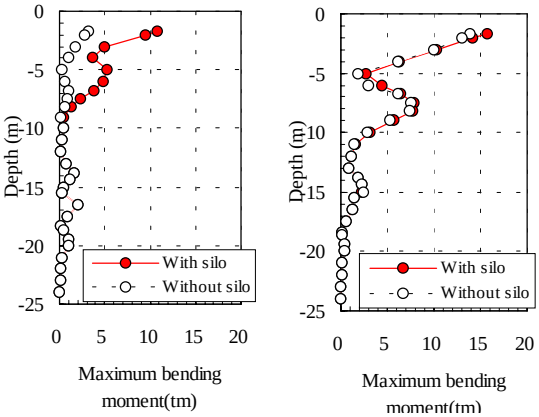

(a) Total stress analysis (b) Effective stress analysis

Fig. 13 Distributions of the bending moment of pile under the condition of rigid connection, in two cases of with silo and without silo

6.4 Influences of inertia force and ground displacement

The distributions of the bending moment of pile under the condition of rigid connection, in two cases: with and without silo cases, are shown in Fig. 13. In the case of TSA, the difference in the bending moments at the pile

head in with and without, is considerable due to the inertia force of silo and its base. Accordingly, inertia force plays more important role than the ground deformation when liquefaction does not occur. On the other hand, in the case of ESA, the difference is negligible. Therefore, ground deformation is dominant in the bending moment of pile when liquefaction occurs.

6.5 Summary of numerical analyses

Numerical analyses clarified that the damage of the pile foundation of the silo induced by the large ground deformation due to liquefaction as well as the inertia force of structure, and that the ground deformation enlarged by liquefaction dominates the pile failure.

7 CONCLUSION

The excavation survey and internal inspection of the damaged piles of silo that suffered severe damage due to the 1993 Hokkaido Nansei-oki earthquake were carried out. The investigation results are concluded as follows:

(1) Damaged portions of the piles were at three different locations: at the pile head, at a depth of 1 to 3 meters below the pile cap, and at the depth corresponding to the bottom of the reclaimed layer. The first two locations are the breakage points of shear failure or bending-shear failure at pile head with rigid pile-cap connection (Type-A) and bending failure at a depth of 1 to 3 meters below sound pile top (Type-B), respectively.

In order to elucidate the causes and mechanism of the pile damage, the dynamic analysis by modeling SSI system into the mass-spring system proposed by Mori et al. (1992) was carried out and the comparison between effective stress analysis (ESA) and total stress analysis (TSA) was demonstrated. The results of the analysis derived the following conclusions:

(2) TSA model can explain the Type-B failure, whereas Type-A failure may be explained by TSA model, however, it can be preferably explained by ESA model. Therefore, liquefaction considerably contributes to causing the damage to the pile heads.

(3) The pile damage at the depth corresponding to the bottom of the reclaimed layer can only be explained by ESA model.

Ground deformation is dominant in the bending moment of pile rather than inertia force when liquefaction occurs.

REFERENCE

Investigation Committee on the 1993 earthquake disasters, JGS (1997), 10.7 Damage to Cement Silo, North Wharf, Hakodate-city, *Investigation Report on the disaster by the 1993 Hokkaido Nansei-Oki earthquake*, The Japanese Geotechnical Society (JGS), pp.406-420 (in Japanese with English abstracts).

Ishihara,K. and Towhata,I.(1980), One-Dimensional Soil Response Analysis during Earthquakes Based on Effective stress Method, *Journal of the Faculty of Enginnering, University of Tokyo(B)*, Vol.35, No.4, pp.655-700.

Mori, S., Ikeda, T., Takimoto, Y., Muto, M.and Tohaya, T. (1992), Influence of Liquefaction on Dynamic behavior of Structure on Piles, *Proceedings of the 10th World Conference of Earthquake Engineering*, pp.1777-1780.

Mori, S. , Numata, A. and Miwa, S. (1994), Feature of liquefaction damage during the 1993 Hokkaido Nansei-oki earthquake, *Proceedings of the 29th Annual Conference of Japanese Society of Soil Mechanics and Foundation Engineering*, pp.1005-1008.

Mori, S and Numata, A. (1994), Liquefaction of Silty Layer filled by dredge during the 1993 Hokkaido Nansei-oki earthquake, *Proceedings of Annual Conference of Architectural Institute of Japan in 1994*, pp.1409-1410 (in Japanese).

Mori, S and Numata, A. (1999), Failure shape of pile heads in a damaged foundation by an earthquake, *Poster Session Proceedings of the 11th Asian Regional Conference on Soil Mechanics and Geotechnical Engineering, Seoul, Korea*, pp.147-148.

Penzien,J., Scheffey,C.F. and Parmelee,R.A. (1964), Seismic Analysis of Bridges on Long Piles, *Journal of the Engineering Mechanics Division, Proceedings of ASCE, Vol.90, No.EM3*, pp.223-254.

Schnabel,P.B., Lysmer,J. and Seed,H.B. (1972), SHAKE-A Computer Program for Earthquake Response Analysis of Horizontally Layered Sites, *Report No. EERC 72-12, Earthquake Engineering Research Center, University of California, Berkeley*.